Dynamical scaling of the structure factor for mesoscopic structures with non-Euclidean fractal morphology

S. Mazumder*
Solid State Physics Division, Bhabha Atomic Research Centre, Mumbai 400 085, India

R. Loidl† and H. Rauch
Atominstitut der Osterreichischen Universitaten, A-1020 Wien, Austria

(Received 24 April 2007; revised manuscript received 13 June 2007; published 23 August 2007)

In order to examine the validity of linear and nonlinear theories on dynamics of new phase formation for mesoscopic structures in non-Euclidean geometry, the real-time evolution of mesoscopic structures of light and heavy water hydrated calcium sulphates has been investigated. Unlike the case for hydration of silicates, hydration of sulphates with light and heavy water does not have distinct characteristic as far as the agreement with the dynamical scaling hypothesis is concerned. There is no change of the topographical mesoscopic structure for hydrating sulphates, unlike silicates, with light and heavy water. Real-time scattering measurements on hydration of sulphates are incomprehensible in the light of observed [S. Mazumder *et al.*, Phys. Rev. Lett. **93**, 255704 (2004); Phys. Rev. B. **72**, 224208 (2005)] results on hydration of silicates. This reports a disagreement with the hypothesis of dynamical scaling of the structure factor of a non-Euclidean system, maintaining same topographical morphology during temporal evolution of the structure. The present investigation, on dynamics of water in different geometric confinements, is also indicative of the fact that the diffusion in non-Euclidean geometry is far from comprehensible.

DOI: 10.1103/PhysRevB.76.064205 PACS number(s): 64.75.+g, 64.90.+b, 61.43.Hv, 61.50.Ks

I. INTRODUCTION

The phenomenon of new phase formation is a representative example of a first order transition. The phenomenon is fundamental and of immense interest as an example of a highly nonlinear process far from equilibrium. The second phase grows with time t and, in late stages, all domain sizes are much larger than all microscopic lengths. In the large time limit, the new phase forming systems exhibit self-similar growth pattern with dilation symmetry, with time-dependent scale, and with the scaling phenomenon.[1] The phenomenon is indicative of the emergence of a morphological pattern of the domains at earlier times, looking statistically similar to a pattern at later times apart from the global change of scale implied by the growth of a time-dependent characteristic length scale $L(t)$—a measure of the time-dependent domain size of the new phase. In the past, extensive investigations on scaling phenomenon in Euclidean geometry have been reported[2–13] in the literature.

The scaling hypothesis assumes the existence of a single characteristic length scale $L(t)$, such that the domain sizes and their spatial correlation are time invariant when the lengths are scaled by $L(t)$. Quantitatively, for isotropic systems, the equal-time spatiotemporal composition modulation autocorrelation function $g(r,t)$, r denoting the spatial coordinate of the system, which reflects the way in which the mean density of the medium varies as a function of distance from a given point, should exhibit the scaling form with time-dependent dilation or scaling symmetry $g(r,t)=f[r/L(t)]$. The scaling function $f[r/L(t)]$ is universal in the sense that it is independent of initial conditions and also of interactions as long as they are short ranged. However, the form of $f[r/L(t)]$ depends nontrivially on n, the number of components in the vector order-parameter field exhibiting the scaling behavior, and d, the dimensionality of the system. The Fourier transform of $g(r,t)$, the structure factor or scattering function $S(q,t)$ for a d dimensional Euclidean system, obeys simple scaling ansatz at late times, $S(q,t)=L(t)^d F[qL(t)]$, where q is the modulus of the scattering vector $\mathbf{q}$. It is important to note that the scaling hypothesis has not been proven conclusively, partially due to the strong nonlinear nature of the problem, except for some model systems. The need for investigations examining the extent and the nature of the validity of the dynamical scaling laws for different physical and geometrical conditions has already been discussed.[14–16] The validity of the dynamical scaling laws for new phase formation in the case of non-Euclidean fractal systems is still an open question.

New phase formation is a diffusion controlled process, but aspects such as diffusion or random walk in non-Euclidean geometry are not satisfactorily comprehensible yet. Diffusion in non-Euclidean fractal geometry is similar, in physical terms, to random walk of drunken messenger on a road system designed by another drunken engineer. In Euclidean geometry, it is established that the curvilinear distance $\langle r(t)\rangle$ covered in time t for a random walk is given by $\sim t^{1/2}$, and the exponent $1/2$ is independent of dimensionality. If it is conjectured that the curvilinear distance covered for a random walk in fractal geometry also behaves as a power law given by $\sim t^{1/2\nu}$—the exact dependence of ν on the fractal geometry is also yet to be established. Monte Carlo simulations for diffusion on the fractal structure generated by random walk on a two-dimensional lattice show[17] $\langle r(t)\rangle \sim t^{\alpha}(\ln t)^{\beta}$, with $\alpha=0.325\pm0.01$ and $\beta=0.35\pm0.03$. For two-dimensional Sierpinski gasket, ν is the ratio of fracton and fractal dimensions.[18] For Sierpinski gasket, both fracton dimension $2[\ln(d+1)/\ln(d+3)]$ and fractal dimension $[\ln(d+1)/\ln 2]$ are uniquely defined by the dimension of em-

bedding Euclidean space—well characterized by one space dimension d. Objects in Euclidean geometry require only the dimension of the embedding Euclidean space for description of their physical properties. However in general, self-similar objects in non-Euclidean geometry require at least three dimensions, namely, embedding Euclidean dimension d, fractal dimension, and spectral or fracton dimension for complete description of various physical quantities. The mass fractal dimension is associated with the heterogeneity and space-filling properties of an object-the smaller the value of fractal dimension the more ramified is the object; surface fractal dimension reflects the roughness of the surface-the higher the value of fractal dimension the more microporous surface is and can be interpreted as the tendency of the surface to spread out into the volume in which it resides, while the fracton or spectral dimension reflects the connectedness of a fractal network. More connectivity between the subunits will lead to higher fracton dimension. For a Euclidean system, the vibrational density of states $\rho(\omega) \sim \omega^{d-1}$ depends on embedding Euclidean dimension d. But for a fractal object, $\rho(\omega) \sim \omega^{\tau-1}$ does not depend on either d or fractal dimension but depends on fracton dimension τ.

Diffusion coefficient in Euclidean geometry is time independent and is expressed as a ratio of the mean squared displacement $\langle r^2(t) \rangle$ and time. In non-Euclidean fractal geometry, mean squared displacement should increase more slowly, and diffusion coefficient will no longer be time independent but rather a decreasing function of time as it leads a drunken messenger into regions of fewer and fewer roads. Exact time dependence of diffusion coefficient in non-Euclidean geometry, in general, is yet to be established. Since the growth of new phase in a phase separating system is a diffusion limited process and diffusion in non-Euclidean geometry is yet an open problem, the related phenomenon of dynamical scaling of structure factor in non-Euclidean geometry is far from comprehensible. The examination, involving real-time kinetics of hydration of silicates with light and heavy water, on the validity of the dynamical scaling phenomenon in non-Euclidean geometry has been reported[14,15] only recently.

It has been observed[14,15] that the kinetics, of hydration of silicates with light and heavy water, is of nonlinear nature even at the initial time. The scattering data could not be interpreted in terms of a linear theory based on the diffusion equation. In the case of hydration of silicates with light water, the hydrating mass exhibits a mass fractal nature throughout hydration, with the mass fractal dimension increasing with time and reaching a plateau. The second phase appears to grow with time initially. Subsequently, the domain size of the second phase saturates. It has also been demonstrated that light water hydration of silicates exhibits a scaling phenomenon for a characteristic length with a different measure. The exhibition of scaling phenomenon for non-Euclidean geometry has been reported for the first time. The temporal behavior of the characteristic length has been observed to be far from a power law.

As far as chemistry is concerned, the hydration of silicates with light and heavy water is expected to be quite similar except for kinetics. Due to different molecular masses of H_2O and D_2O, diffusion is expected to be more sluggish for D_2O. However, some incomprehensible contrasting behavior has been observed in the case of hydration of silicates with heavy water as far as the kinetics of new phase formation is concerned. The domain size of the density fluctuations grows in the beginning for a while, and subsequently, appears to shrink with time, reaching saturation ultimately. In the case of hydration of silicates with heavy water, the microstructure of the hydrating mass undergoes a transition from mass fractal to surface fractal, and subsequently, to mass fractal. The scaling phenomenon, with all possible measures of the characteristic length, has not been established for the hydration kinetics with heavy water. It is only a conjecture at this stage that the different rates of diffusion of light and heavy water in forming a gel structure in silicates lead to the formation of different structural networks with different scattering contrasts. We are unable to put forward a more conclusive reason even now.

In view of the observed contrasting behavior of hydration of silicates with light and heavy water, it was considered worth examining the uniqueness of silicates in cementitious material to exhibit this contrasting behavior. In the present experiment of hydration of sulphates with light and heavy water, the similar contrasting behavior of hydration has not been observed. However, present observations are fascinating and shed some light to the phenomenon of dynamical scaling of structure factor for fractal geometry.

This work reports the mesoscopic structural investigations on real-time hydration of plaster of Paris ($CaSO_4\frac{1}{2}H_2O$, calcium sulphate hemihydrate) to gypsum ($CaSO_4 \cdot 2H_2O$). The hydration reaction can be written as

$$2CaSO_4 \cdot \tfrac{1}{2}H_2O + 3H_2O \rightarrow 2CaSO_4 \cdot 2H_2O.$$

The above hydration reaction is extremely slow and that is why calcium sulphate hemihydrate is added in Portland cements to retard the hydration process. Gypsum ($CaSO_4 \cdot 2H_2O$) crystals are needle shaped, which lock in water molecules and generate a solid structure.

Cement is a material which binds together solid bodies, called aggregates, by hardening from a plastic state arising from mixing with water. Cement, commonly used in construction industry and in nuclear energy program for immobilization of non-heat-generating low level radioactive waste, is a composite material consisting of fine grains of calcium silicates and aluminates. Gypsum plaster ($CaSO_4 \cdot 2H_2O$), also termed as plaster of Paris, is also a cement used mainly for fine polishing work. Cement functions by forming a plastic paste initially when mixed with water, which develops rigidity, termed as setting, and then steadily increases in compressive strength, termed as hardening, by chain reaction with water, termed as hydration. Setting and hydration determine the strength and the dimensional stability of a cement composite. The understanding of the mechanism by which a newly mixed cement turns into a gel structure, rendering required rigidity and compressive strength, remains far from being understood despite the existence of two main theories[19] explaining the hardening of silicate cements. The complexity arises mainly due to poor understanding of the hydration kinetics and physical nature of the hydration prod-

ucts. Understanding setting and hydration may contribute to the improvement of the quality of this important material.

On mixing cement and water, a complex series of hydration reactions take place of which the main products are an amorphous calcium-silicate-hydrate gel-like structure and crystalline calcium hydroxide, which accounts for 20% of the volume of hydrated material in aged cement.

The successful large-scale use of cement depends principally on two aspects of cement-water reaction:

(i) There is a so-called dormant period during which rates of hydration are low and a substantial part of the mixture retains sufficient plasticity for proper placing and compaction.

(ii) The hydration products formed after setting progressively fill the space previously occupied by the water, giving a dense structure with no undesirable overall volume change. The unoccupied space remains as pores of mesoscopic, 1–1000 nm, dimension. The two phase system thus formed consists of solids and pores separated by random surfaces.

Elastic properties of two phase porous solids are dictated by the degree of continuity of the solid, while the transport property such as permeability is governed by the connectivity of the pores. The interface, separating the solids from pores, and its geometry affect transport properties through the solid, and are receiving experimental attention only recently. Scattering technique such as small-angle scattering can probe interfaces of closed as well as open pores of mesoscopic dimensions. It is not possible to access closed pores by means of conventional laboratory based technique such as mercury porosimetry.

II. EXPERIMENT

Powder specimens of analytical grade calcium sulphate hemihydrate were mixed with heavy water (D_2O) and double distilled light water (H_2O) at varying water/cement (w/c) ratio, by mass, ranging approximately from 0.6 to 0.7, to obtain a pastelike mass. For scattering measurements, approximately 0.08 ml of the freshly prepared paste was spread in a circular hole of 10 mm diameter punched on a cadmium sheet of nearly 1.0 mm thickness. The counting time of one complete scattering curve was about 6 min for real-time measurements on hydrating samples, varying with medium (H_2O/D_2O) of hydration and w/c ratio.

A preliminary measurement with a medium resolution small-angle neutron scattering (SANS) facility[20] indicated that hydrated plaster of Paris (PP) has a fractal microstructure on the length scale of 1–100 nm. It also indicated the possibility of existence of inhomogeneities larger than 100 nm. So SANS measurements were carried out with ultrasmall angle neutron scattering instrument[21] S18 at 58 MW high flux reactor at ILL, France. The wavelength λ used was 1.87 Å. The scattered intensities were recorded as a function of q [$=4\pi(\sin\theta)/\lambda$, 2θ being the scattering angle and q is the modulus of the scattering vector $\mathbf{q}$]. The scattering data were corrected for background and primary beam geometry. For background, scattering measurements have been carried out at about $q=10^{-2}$ Å^{-1}. Background was relatively higher for light water hydrating specimens but for all the experimental specimens measured, background was insignificantly smaller in comparison with the recorded signal. At the outset, it was inferred that hydrating specimens are isotropic in nature and so is the scattering function[22] $S(q,t)$.

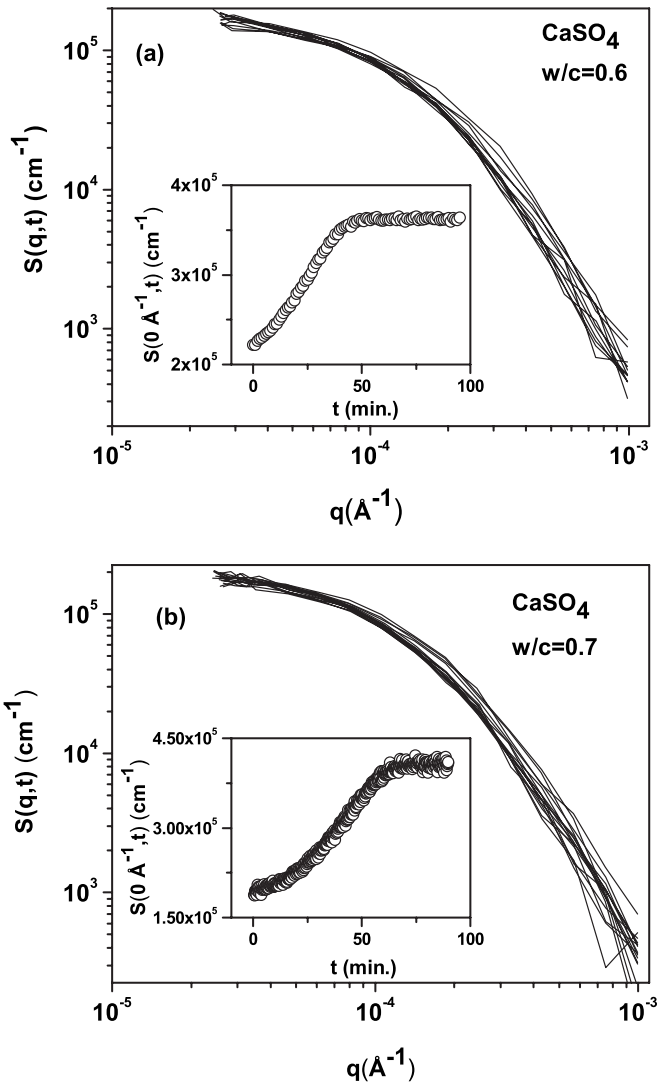

FIG. 1. Time evolution of scattering function $S(q,t)$ for light water hydrating plaster of Paris with $w/c=0.6$ and $w/c=0.7$ by mass, respectively. The inset shows the time evolution of $S(0\ \text{Å}^{-1},t)$. Statistical error bars are smaller than the respective symbol sizes.

III. DATA INTERPRETATION AND DISCUSSION

Figure 1 depicts the time t evolution of scattering function $S(q,t)$ in absolute scale for light water hydrating PP with $w/c=0.6$ and $w/c=0.7$, respectively. It is evident from Fig. 1 and more apparent from the inset of Fig. 2 that with increasing hydration time, the curvature of the scattering profiles in the vicinity of $q\rightarrow 0$ varies nonlinearly, indicating the nonlinearity in the growth of pores. The curvature $\kappa(t)$ of normalized $S(q,t)$ at q is given by

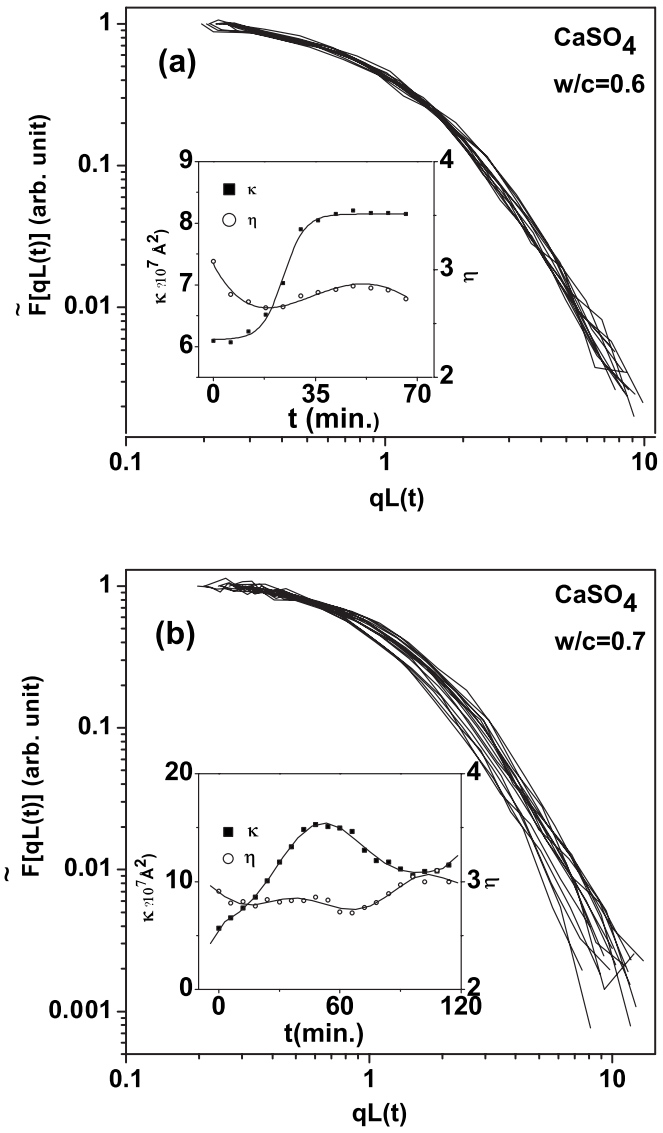

FIG. 2. Scaled scattering function $\tilde{F}[qL(t)]$ for light water hydrating plaster of Paris with $w/c=0.6$ and $w/c=0.7$ by mass, respectively. The inset shows the time evolution of $\kappa(t)$ and $\eta(t)$. Statistical error bars are smaller than the respective symbol sizes. The solid lines are only guides for the eyes.

$$\kappa(t) = \frac{|d^2[S(q,t)/S(0,t)]/dq^2|}{(1+\{d[S(q,t)/S(0,t)]/dq\}^2)^{3/2}}.$$

The curvature[23] $\kappa(t)$ in the vicinity of $q \to 0$ of a scattering profile $S(q,t)$ is related to

$$G(t) = -d(\ln[S(q,t)/S(0,t)])/dq^2,$$

where $G(t)$ is the negative gradient of the Guinier plot of the normalized scattering profile. For a single scattering profile from monodisperse population of spheres of radius R, in the vicinity of $q \to 0$, $\kappa = 2R^2/5$, whereas $G = R^2/5$. In subsequent discussions, κ is defined in the vicinity of $q \to 0$ only throughout if not mentioned otherwise. For a polydisperse population of spherical scatterers, with number density $\rho(R)$ for scatterers of radius R, having the same scattering length density difference, $\kappa = 2\langle R^8\rangle/5\langle R^6\rangle$, where $\langle R^n\rangle$ is the nth moment of the distribution $\rho(R)$. Curvature[23] and radius of curvature are reciprocal to each other.

It is a specialty of ultrasmall angle neutron scattering instrument[21] that one can measure scattering at $q=0$ Å^{-1} by aligning the analyzer crystal perfectly parallel to the monochromator crystal and recording the scattering signal. The insets of Fig. 1 show the time evolution of $S(0\ \text{Å}^{-1},t)$ in absolute scale, where real time measurement on scattering function $S(q,t)$ at $q=0$ Å^{-1} has been carried out by keeping the analyzer crystal stationary and recording the scattering data with a short interval of measurement time. From the inset of Fig. 1, it is evident that $S(0\ \text{Å}^{-1},t)$ vs t has a shoulder at about $t \approx 50$ min for hydrating specimen with $w/c=0.6$ and at about $t \approx 70$ min for hydrating specimen with $w/c=0.7$. The broad characteristic features of $S(0\ \text{Å}^{-1},t)$ vs t for light water hydrating sulphates have been observed to be quite similar to those observed for light water hydrating silicates. $S(0\ \text{Å}^{-1},t)$ varies linearly with time in two discrete domains of time (approximately $t \leqslant 50$ min and $t \geqslant 50$ min, respectively, for hydrating specimen with $w/c=0.6$) with distinct slopes. Two linear regions separated by a curved region are termed as shoulder. Real-time measurements of scattering function $S(q,t)$ at constant q have been carried out at two other discrete q values ($q \approx 0.000\ 14$ Å^{-1} and $q \approx 0.000\ 32$ Å^{-1}). The qualitative feature of $S(0.000\ 14\ \text{Å}^{-1},t)$ vs t is similar to $S(0\ \text{Å}^{-1},t)$ vs t inclusive of the position of the shoulder. However, $S(0.000\ 32\ \text{Å}^{-1},t)$ vs t is dissimilar in nature vis-à-vis $S(0\ \text{Å}^{-1},t)$ vs t, and apparently has sinusoidal variation. For brevity, these figures are not presented here.

The insets of Fig. 2 depict the time evolution of $\kappa(t)$ for light water hydrating PP with $w/c=0.6$ and $w/c=0.7$, respectively. For hydrating specimen with $w/c=0.6$, $\kappa(t)$ increases with time initially rather slowly, intermediately rapidly, and finally reaches a plateau. It is to be noted that for monodisperse population of inhomogeneity, the linear dimension of the inhomogeneity is proportional[23] to $\sqrt{\kappa(t)}$. However, for specimen with $w/c=0.7$, $\kappa(t)$ increases with time initially almost linearly, reaches a maximum, and finally comes down. However, from the present set of experiments, we cannot conclude about the asymptotic temporal variation of $\kappa(t)$. Unlike the case for hydration of silicates, no systematics has been observed as far as the temporal variation of $\kappa(t)$ for hydration of sulphates varying with w/c ratio. It is pertinent to recall[14,15] that hydration of silicates with light water $\kappa(t)$ vs t has similar generic variation irrespective of w/c ratio.

The insets of Fig. 2 also depict time evolution of Porod exponent $\eta(t)$, as estimated from $\ln[S(q,t)]$ vs $\ln(q)$ in the q range of 0.000 25–0.001 Å^{-1}, for light water hydrating PP with $w/c=0.6$ and $w/c=0.7$, respectively. Porod exponent for all the light water hydrating specimens lies in the range of 2–3, indicating the mass fractal nature of the hydrating paste. For objects whose volume or mass is fractal (cluster aggregates), $S(q,t)$ asymptotically approaches a form $S(q,t) \sim q^{-\eta}$, where the exponent η reflects[24] directly the mass fractal dimension D_m. For a mass fractal object embedded in a three-dimensional space, $\eta = D_m$ with $1 < \eta < 3$ and

$1<D_m<3$. Like mass fractal objects, there are surface fractal objects[25] with uniform internal density but with outer surface exhibiting self-similar geometric properties. For a surface fractal object with surface fractal dimension D_s $3<\eta<4$ and $2<D_s<3$. When the mass fractal becomes space filling, both mass and surface fractal dimensions tend to the value 3 and $S(q,t)$ asymptotically approaches[26] a form $S(q,t)\sim q^{-3}$. Then, when mass consolidates itself on a length scale larger than q^{-1} and the surface stays rough, structures undergo transition[26] to a surface fractal regime and Porod exponent η becomes greater than 3. For a mass fractal cluster with size ξ and fractal dimension D_m, R_G (the Guinier radius) and ξ are related by[26] $(R_G/\xi)^2=\frac{1}{2}D_m(D_m-1)(D_m+1)$.

It is evident from the insets of Fig. 2 that the mass fractal dimension of the light water hydrating sulphates has sinusoidal variation with hydration time irrespective of w/c ratio. The sinusoidal variation of $\eta(t)$ with time does not explain the increasing compressive strength of hydrating specimen with time. The increasing compressive strength is perhaps associated with decreasing lacunarity[15] with time. It is only a conjecture at this stage, and we are unable to shed more light for time being.

Furthermore, unlike the case of light water hydration of silicates, the generic variation of $\kappa(t)$ vs t and $\eta(t)$ vs t differs widely in the case of light water hydration of sulphates. For hydration of silicates[14,15] with light water, the qualitative patterns of the time evolution of $\kappa(t)$ and $\eta(t)$ are the same irrespective of w/c ratio. For hydration of silicates with light water, irrespective of w/c ratio, both $\kappa(t)$ and $\eta(t)$ increase with time initially almost linearly and reaches a plateau, finally yielding similar generic temporal variation.

In accordance with the linear theory[27] of new phase formation, temporal variation of scattering function $S(q,t)$ is given by

$$S(q,t)=S(q,0)\exp[2t\alpha(q)],$$

where $\alpha(q)$ is the time-independent proportionality constant.

It has been observed that $\alpha(q)$ does not behave independent of time for all the hydrating specimen, as discussed in this paper, even at the initial stage of the measurements, indicating inadequacy of the linear theory to comprehend the observations of the present set of measurements.

In order to examine the scattering function kinetics in the light of dynamical scaling phenomenon, based on nonlinear theories[1] of new phase formation, the normalized scaling function $\tilde{F}[qL(t)]=S(q,t)[L(t)]^{-D_m}/\Sigma q^{D_m}S(q,t)\ \delta q$ has been calculated, where $L(t)=\sqrt{\kappa(t)}$, $L(t)=\xi(t)$ [$\xi(t)$ estimated by fitting scattering function $S(q,t)$ with that for a fractal object[26]], and δq is the experimental q increment. For brevity, the results obtained with $L(t)=\xi(t)$ are not presented here as these were qualitatively similar to those obtained for $L(t)=\sqrt{\kappa(t)}$.

It is important to note that for a mass fractal object, surface area also scales[25] as R^{D_m} for a spherical surface of radius R. The plots of $\tilde{F}[qL(t)]$ for light water hydrating PP with $w/c=0.6$ and $w/c=0.7$ are shown in Fig. 2. It is evident from the figure that the scaling functions are not strictly time independent, indicating poor agreement with the scaling hypothesis. These results are in sharp contrast to those observed[14,15] in the case of light water hydrating specimens of silicates. In the case of hydrating silicates, good agreement with scaling hypothesis has been observed for a wide range of w/c ratio. It has also been observed that scaling phenomenon is also not operative for all the light water hydrating sulphate specimens under investigation for $L(t)=[q_1(t)]^{-1}$, where $q_1(t)$ is the first moment of the scattering function $S(q,t)$.

Having observed[14,15] sharp contrasting features of the kinetics of hydration of silicates with light water and heavy water, it was worth considering to repeat the scattering experiments on hydration of sulphates with heavy water. It is also important to note that as far as chemistry is concerned, the hydration of cement with light and heavy water is expected to be quite similar except for kinetics. However, the density fluctuations as probed by small-angle scattering experiments will have different scattering contrasts when hydrated with light water and heavy water. Further, in a porous medium, water may form small pools inside some pores, giving rise to very different contrasts. However, dynamical scaling phenomenon in a multicomponent system may arise even when the inhomogeneities are polydisperse in nature. The polydispersity may arise due to varying sizes, shapes, and contrasts.

The observations from scattering experiments on heavy water hydrating plaster of Paris with $w/c=0.6(20/18)$ and $w/c=0.7(20/18)$ will be dealt with now. It is pertinent to note that heavy water hydrating cement with $w/c=x(20/18)$ will have the same molar ratio of water and cement as in light water hydrating cement with $w/c=x$.

Figure 3 depicts the time evolution of scattering function $S(q,t)$ for heavy water hydrating PP with $w/c=0.6(20/18)$ and $w/c=0.7(20/18)$ respectively. It is evident from Fig. 3 and more apparent from the inset of Fig. 4 that with increasing hydration time, the curvature of the scattering profiles in the vicinity of $q\rightarrow 0$ has somewhat damped oscillatory behavior, indicating oscillatory temporal variation of the linear dimension of the inhomogeneity.

The insets of Fig. 3 show the time evolution of $S(0\ \text{Å}^{-1},t)$ in absolute scale. The characteristic features of $S(0\ \text{Å}^{-1},t)$ vs t for heavy water hydrating sulphates have been observed to be quite different both from those observed for light water hydrating sulphates and heavy water hydrating silicates. Before carrying out the experiment, we were expecting that saturation of $S(0\ \text{Å}^{-1},t)$ for heavy water hydrating specimen will be somewhat delayed due to relatively slower diffusion of D_2O. However, unlike the case for light water hydrating sulphate specimens, $S(0\ \text{Å}^{-1},t)$ vs t has two shoulders at $t\approx 25$ min and $t\approx 60$ min, respectively, for heavy water hydrating specimen with $w/c=0.6(20/18)$, and at $t\approx 50$ min and $t\approx 100$ min, respectively, for hydrating specimen with $w/c=0.7(20/18)$. In fact, even the qualitative features of $S(0\ \text{Å}^{-1},t)$ vs t differ in detail for heavy water hydrating specimens varying with w/c ratio. For heavy water hydrating specimen with $w/c=0.6(20/18)$, $S(0\ \text{Å}^{-1},t)$ increases linearly initially, reaches a short-lived plateau at $t\approx 25$ min, and increases further on to reach a long-lived plateau at t

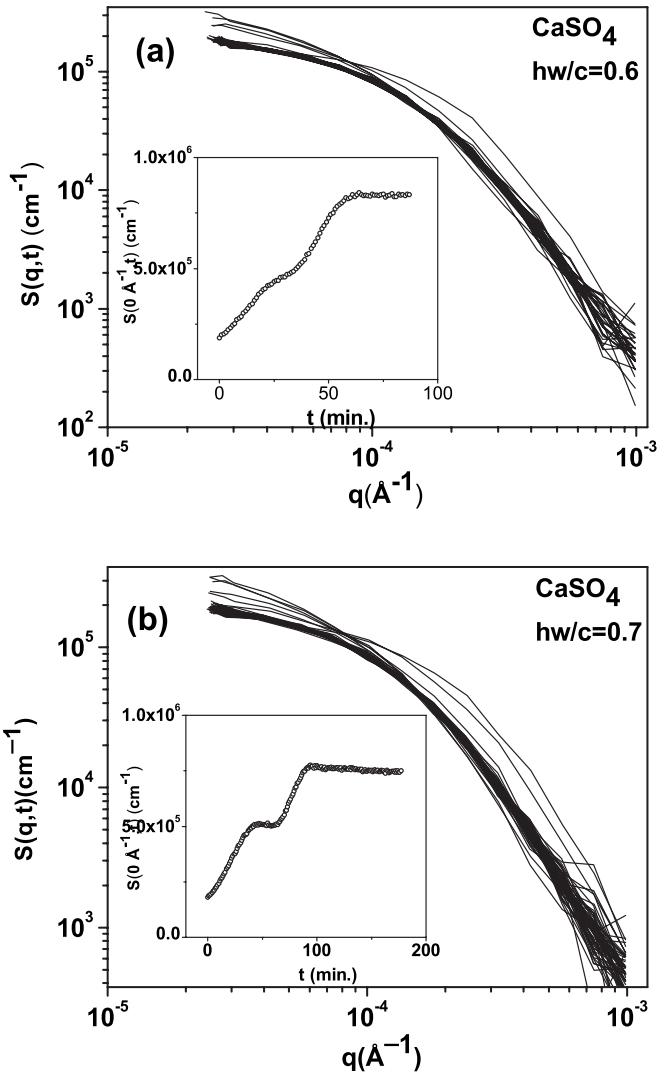

FIG. 3. Time evolution of scattering function $S(q,t)$ for heavy water hydrating plaster of Paris with $w/c=0.6(20/18)$ and $w/c=0.7(20/18)$ by mass, respectively. The inset shows the time evolution of $S(0\ \text{Å}^{-1},t)$. Statistical error bars are smaller than the respective symbol sizes.

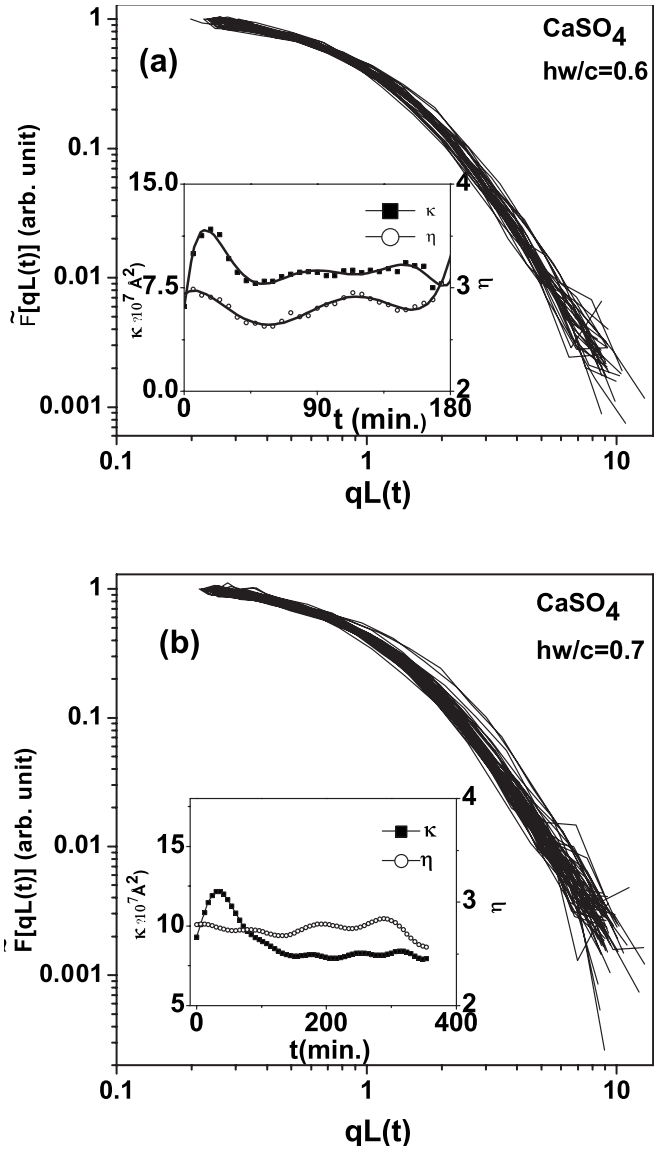

FIG. 4. Scaled scattering function $\tilde{F}[qL(t)]$ for heavy water hydrating plaster of Paris with $w/c=0.6(20/18)$ and $w/c=0.7(20/18)$ by mass, respectively. The inset shows the time evolution of $\kappa(t)$ and $\eta(t)$. Statistical error bars are smaller than the respective symbol sizes. The solid lines are only guides for the eyes.

≈ 60 min. However, for heavy water hydrating specimen with $w/c=0.7(20/18)$, $S(0\ \text{Å}^{-1},t)$ increases linearly initially with time and reaches an intermediate plateau at $t\approx 50$ min. The lifetime of the plateau is about 20 min. $S(0)\ \text{Å}^{-1},(t)$ increases then on until about 100 min and continuously decreases further on with a marginal negative slope.

The insets of Fig. 4 depict the time evolution of $\kappa(t)$ for heavy water hydrating PP with $w/c=0.6(20/18)$ and $w/c=0.7(20/18)$, respectively. Similar to the case of hydration of silicates, systematics has been observed, as far as the temporal variation of $\kappa(t)$ for heavy water hydration of sulphates, to vary with w/c ratio. Irrespective of w/c ratio, temporal variation of $\kappa(t)$ has damped oscillatory behavior, indicating damped oscillatory behavior of the temporal behavior of the linear dimension of the inhomogeneity.

The insets of Fig. 4 also depict time evolution of Porod exponent $\eta(t)$, as estimated from $\ln[S(q,t)]$ vs $\ln(q)$ in the q range of 0.000 25–0.001 Å^{-1}, for light water hydrating PP with $w/c=0.6(20/18)$ and $w/c=0.7(20/18)$, respectively. Similar to the case of hydration of sulphates with light water, Porod exponent $\eta(t)$ for all the heavy water hydrating specimens lies in the range of 2–3 indicating the mass fractal nature of the hydrating paste. Like the case of hydration of sulphates with light water, the mass fractal dimension or the degree of ramification of the heavy water hydrating sulphates has sinusoidal variation with hydration time irrespective of w/c ratio. $\eta(t)$ vs t has no sharp distinctive feature with varying medium (H_2O/D_2O) of hydration and varying w/c ratio.

Like the case of light water hydration of sulphates and unlike the case of hydration of silicates, the generic variation of $\kappa(t)$ vs t and $\eta(t)$ vs t differs widely in the case of heavy water hydration of sulphates.

In order to examine the validity of the scaling hypothesis for the case of hydration of sulphates with heavy water, the normalized scaling function $\tilde{F}[qL(t)]=S(q,t)[L(t)]^{-D_m}/\Sigma q^{D_m}S(q,t)\ \delta q$ has been calculated, where $L(t)=\sqrt{\kappa(t)}$ and δq is the experimental q increment. The plots of $\tilde{F}[qL(t)]$ for heavy water hydrating PP with $w/c=0.6(20/18)$ and $w/c=0.7(20/18)$ are shown in Fig. 4. It is evident from the figure that the scaling functions are not strictly time independent, indicating poor agreement with the scaling hypothesis. These results are similar to those observed for the case of hydration of sulphates with light water. It has also been confirmed that scaling phenomenon is also not operative for all the heavy water hydrating sulphate specimens under investigation for $L(t)=[q1(t)]^{-1}$, where $q_1(t)$ is the first moment of the scattering function $S(q,t)$.

A consequence of the scaling hypothesis is that the unnormalized nth moment of the structure factor behaves as

$$S_n(t) = \int q^n S(q,t)dq = \int [qL(t)]^n F[qL(t)]d[qL(t)] \quad (1)$$

and

$$q_n(t) \equiv S_n(t)/S_0(t) \propto L^{-n}(t). \quad (2)$$

It is considered prudent to examine the extent of validity of scaling hypothesis experimentally, manifested through Eqs. (1) and (2), since accurate measurements of the structure factor is possible only over a restricted range of wave vector. The long-wavelength cutoff in the structure factor introduces errors in the lower moments, particularly at later times, whereas the short-wavelength cutoff affects the higher-order moments. From Fig. 5, it is evident that there is no striking difference, unlike the case of hydration of silicates, in the temporal variation of the ratio q_2/q_1^2 for light water and heavy water hydrated specimens of PP. The measured integrated intensity $S2(t)$, proportional to the volume fraction of the new phase, is time dependent and is therefore responsible for the stronger time dependence of the ratio $S_0(t)/S_1^2(t)$. Figure 5 depicts the variation of $S_2(t)$ with time for the hydrating specimens of PP with $w/c=0.6$ and $w/c=0.7$, respectively. The time dependence of the moment ratios is quite similar, as evident from Fig. 5, for light and heavy water hydrating specimens. These results are strikingly different for the case of hydration of silicates.

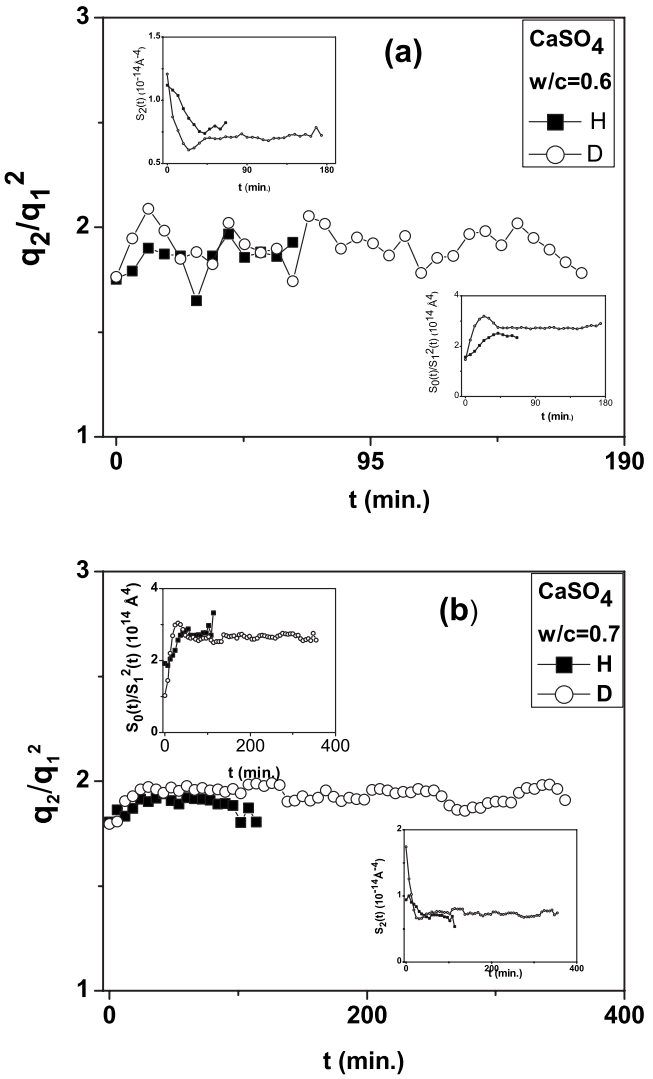

FIG. 5. Time evolution of q_2/q_1^2 for heavy and light water hydrating plaster of Paris. For light water hydrating specimen, water/cement ratios are given by $w/c=0.6$ and $w/c=0.7$, respectively. For heavy water hydrating specimen, water/cement ratios are given by $w/c=0.6(20/18)$ and $w/c=0.7(20/18)$, respectively. Inset (1) shows the time evolution of $S_2(t)$, while inset (2) shows the time evolution of $S_0(t)/S_1^2(t)$. Statistical error bars are smaller than the respective symbol sizes. The solid lines are only guides for the eyes.

IV. CONCLUSIONS

In the present work, temporal evolution of mesoscopic structure and hydration kinetics of sulphates with light and heavy water has been investigated. The experimental observations have been compared with the corresponding observations with silicates. Similarities and dissimilarities between the hydration characteristics of silicates and sulphates have been highlighted. In view of the contrasting behavior as far as the kinetics of hydration of silicates with light and heavy water is concerned, it was considered worth examining the uniqueness of silicates in cementitious material to exhibit this contrasting behavior. However, for hydration of sulphates with light and heavy water, similar contrasting behavior of hydration has not been observed. The observations are completely incomprehensible. It is only a conjecture at this stage that effect such as hydrogen bonding may be playing some role. The spectacular observations also point to the gray area of our understanding of the hydration of cement. The poor understanding of both the hydration kinetics and the physical nature of hydration products became glaringly evident. It is only pertinent to note here that intracellular water dynamics in biological systems also yields fascinating surprises.[28]

For the case of hydration of silicates with light water, hydrating mass remains mass fractal throughout—no topographical change of the hydrating mass as a function of time and scaling phenomenon has been observed. For the case of

hydration of silicates with heavy water, hydrating mass undergoes transition from mass fractal to surface fractal to mass fractal—a topographical change of the hydrating mass as a function of time. Scaling phenomenon has also not been observed for hydration of silicates with heavy water. So it was conjectured that the topographical change of the hydrating mass could be the plausible reason why dynamical scaling was not observed in the case of hydration of silicates with heavy water. However, such an important conclusion needs further scrutiny. So we chose the real-time mesoscopic structural investigation of hydration of sulphates considering the fact that the new chemical environment will shed light on the aforementioned conclusion.

The present reported observations show that both for light and heavy water hydration of sulphates, time evolution of the scattering functions do not exhibit scaling phenomenon for a characteristic length with any possible measure, although there is no topographical change of the hydrating mass as a function of time. Hydrating mass remains mass fractal throughout. The present investigation clearly indicates disagreement with the hypothesis of dynamical scaling of structure factor for fractal systems without temporal topolographical change. The present investigation also indicates that temporal evolution of mesoscopic structure of hydrating cementitious material is far from being understood and deserves intense scrutiny. The present paper is a step forward, in our understanding, in the phenomenon of dynamical scaling of structure factor in non-Euclidean geometry.

ACKNOWLEDGMENT

We are extremely grateful to our colleagues, who have reviewed this paper, for many useful suggestions.

*Corresponding author. FAX: 91-22-25505151; smazu@barc.gov.in
†Also at Institut Laue-Langevin, Grenoble, France.

[1] A. J. Bray, Adv. Phys. **43**, 357 (1994), and references therein.
[2] S. Katano and M. Iizumi, Phys. Rev. Lett. **52**, 835 (1984).
[3] M. Furusaka, Y. Ishikawa, and M. Mera, Phys. Rev. Lett. **54**, 2611 (1985).
[4] S. Mazumder, D. Sen, I. S. Batra, R. Tewari, G. K. Dey, S. Banerjee, A. Sequeira, H. Amenitsch, and S. Bernstorff, Phys. Rev. B **60**, 822 (1999).
[5] R. Tewari, S. Mazumder, I. S. Batra, G. K. Dey, and S. Banerjee, Acta Mater. **48**, 1187 (2000).
[6] D. Sen, S. Mazumder, R. Tewari, P. K. De, H. Amenitsch, and S. Bernstorff, J. Alloys Compd. **308**, 250 (2000).
[7] C. V. Santilli, S. H. Pulcinelli, and A. F. Craievich, Phys. Rev. B **51**, 8801 (1995).
[8] P. Fratzl, J. Appl. Crystallogr. **24**, 593 (1991).
[9] F. Langmayr, P. Fratzl, and G. Vogl, Acta Metall. Mater. **40**, 3381 (1992).
[10] E. Velasco and S. Toxvaerd, Phys. Rev. Lett. **71**, 388 (1993).
[11] A. P. Y. Wong, P. Wiltzius, and B. Yurke, Phys. Rev. Lett. **68**, 3583 (1992).
[12] A. P. Y. Wong, P. Wiltzius, R. G. Larson, and B. Yurke, Phys. Rev. E **47**, 2683 (1993).
[13] M. Rao and A. Chakrabarti, Phys. Rev. E **49**, 3727 (1994).
[14] S. Mazumder, D. Sen, A. K. Patra, S. A. Khadilkar, R. M. Cursetji, R. Loidl, M. Baron, and H. Rauch, Phys. Rev. Lett. **93**, 255704 (2004).
[15] S. Mazumder, D. Sen, A. K. Patra, S. A. Khadilkar, R. M. Cursetji, R. Loidl, M. Baron, and H. Rauch, Phys. Rev. B **72**, 224208 (2005).
[16] S. Mazumder, Physica B **385–386**, 7 (2006).
[17] R. Dekeyser, A. Maritan, and A. Stella, Phys. Rev. Lett. **58**, 1758 (1987).
[18] R. Rammal and G. Toulouse, J. Phys. (Paris), Lett. **44**, L13 (1983).
[19] F. M. Lea, *The Chemistry of Cement and Concrete* (Arnold, London, 1956).
[20] S. Mazumder, D. Sen, T. Saravanan, and P. R. Vijayaraghavan, J. Neutron Res. **9**, 39 (2001).
[21] M. Hainbuchner, M. Villa, G. Kroupa, G. Bruckner, M. Baron, H. Amenitsch, E. Seidl, and H. Rauch, J. Appl. Crystallogr. **33**, 851 (2000).
[22] L. Van-Hove, Phys. Rev. **95**, 249 (1954).
[23] S. Mazumder, D. Sen, S. K. Roy, M. Hainbuchner, M. Baron, and H. Rauch, J. Phys.: Condens. Matter **13**, 5089 (2001); N. Pishkunov, *Differential and Integral Calculus* (Mir, Moscow, 1974), p. 208, english translation.
[24] T. Freltoft, J. K. Kjems, and S. K. Sinha, Phys. Rev. B **33**, 269 (1986); J. Teixeira, in *On Growth and Form*, edited by H. E. Stanley and N. Ostrowsky (Kluwer Academic, Dordrecht, 1986), pp. 145–162.
[25] P. Pfeifer and D. Avnir, J. Chem. Phys. **79**, 3558 (1983); **80**, 4573(E) (1984).
[26] S. K. Sinha, Physica D **38**, 310 (1989).
[27] J. W. Cahn, Acta Metall. **9**, 795 (1961).
[28] M. Tehei, B. Franzetti, K. Wood, F. Gabel, E. Fabiani, M. Jasnin, M. Zamponi, D. Oesterhelt, G. Zaccai, M. Ginzburg, and B. Ginzburg, Proc. Natl. Acad. Sci. U.S.A. **104**, 766 (2007).